J. Chem. Sci. Vol. 127, No. 9, September 2015, pp. 1523–1530.
DOI 10.1007/s12039-015-0926-7

One-pot Solvent-free Catalytic Dimerization Reaction of Phenylacetylene to 1-Phenylnaphthalene

AVAT (ARMAN) TAHERPOUR[a,b,*], SEPEHR TABAN[c] and AKO YARI[a]

[a]Department of Organic Chemistry, Faculty of Chemistry, Razi University, P.O. Box: 67149-67346, Kermanshah, Iran

[b]Medical Biology Research Center, Kermanshah University of Medical Sciences, Kermanshah, Iran

[c]Chemistry Department, Science Faculty, Islamic Azad University, Arak Branch, P.O. Box 38135-567, Arak, Iran

e-mail: avatarman.taherpour@gmail.com

MS received 21 September 2014; revised 28 April 2015; accepted 29 April 2015

Abstract. In this study, we report a smooth one-pot, solvent-free catalytic dimerization of phenylacetylene (**1**) to 1-phenylnaphthalene (**2**) by Cu/C at room temperature in good yield (∼100%). In the computational study, the structure of the 1-phenylnaphthalene was optimized by DFT-B3LYP/6-31G* method. The rotation barrier around C-C of the phenyl and naphthalene parts of the molecule and its UV-Visible spectrum were calculated. The modelling of the mechanism of production of **2** from **1** was performed with and without Cu/C catalyst. The data of EDS and SEM of the Cu/C catalyst surface are also reported.

Keywords. Catalytic reactions; Phenylacetylene; 1-Phenylnaphthalene; Copper(0)-Carbone catalyst; Solvent free synthesis; EDS; SEM; Molecular modelling.

1. Introduction

Polycyclic aromatic hydrocarbons (PAHs) have been attracting a lot of attention in recent years.[1–6] They are formed as a result of burning organic compounds and in natural thermal geological reactions. PAHs occur in oil, coal, and tar deposits, and are produced as by-products of fuel burning (fossil fuel or biomass).[1–3] PAHs are found primarily in soil, sediment and oily substances, as opposed to water or air.[4] 1-phenylnaphthalene was prepared by the reaction of α-halonaphthalenes with mercury diphenyl,[7a,b] or with benzene in the presence of aluminum chloride,[7a,b] and by means of a Grignard synthesis, starting with either bromobenzene, or cyclohexyl chloride and α-tetralone,[7a,c,d] or with α-bromonaphthalene and cyclohexanone.[7a,c-e] A 60% yield is reported for the Grignard preparation from cyclohexanone.[7a,g] The formation of the hydrocarbon through the diazo reaction,[7a,g-j] appears to be less attractive than the described method. Dehydrogenation of the reduced naphthalene is accomplished by the use of sulfur,[7a,c] bromine,[7a,e] platinum black, or selenium.[7a,b] 1-Phenylnaphthalene has also been prepared by oxidation of 1-Phenyldialin.[7a]

An efficient organocatalytic method for constructing biaryls through aromatic C-H activation is reported by Sun *et al.* in 2010.[8] They have described the identification of a cross-coupling between aryl iodides/bromides and the C–H bonds of arenes that is mediated solely by the presence of 1,10-phenanthroline as catalyst in the presence of KO*t*-Bu as a base. This apparently transition metal-free process provides a new strategy to achieve direct C–H functionalization.[8]

In 2011, the dimerization reaction of phenylacetylene (**1**) in presence of Pd(0) nanoparticles was reported by Firuzabadi *et al.*[9] In this reaction 1,4-diphenyl-but-1-en-3-yne was produced. It is demonstrated in that report that the nanoparticles show high catalytic activity for the Sonogashira–Hagihara coupling reaction of various aryl halides as well as heteroaryl halides and also β-bromo styrene with phenylacetylene under copper-, ligand- and amine-free conditions.[9–14] It is also reported that the reactions were carried out at 100°C in molten tetrabutylammonium bromide (TBAB) or polyethylene glycol in the presence of potassium acetate as a base in argon atmosphere. Dimerization of phenylacetylene in similar conditions in air was also previously described by Firuzabadi *et al*.[9]

The dimerization of arylethynes catalyzed by vanadium phthalocyanine to give substituted biaryls have been previously investigated.[15] In 2009, the dimerization

*For correspondence

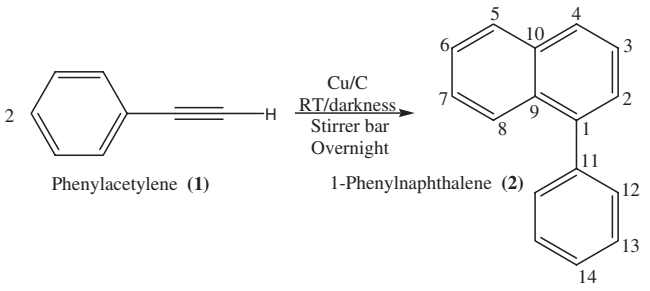

Figure 1. One-pot, solvent-free catalytic dimerization of phenylacetylene **(1)** to 1-phenylnaphthalene **(2)** by Cu/C at room temperature.

reaction of *para*-Cl-phenylacethylene in presence of vanadium phthalocyanine was reported by Cicero *et al.*[15] The reaction had produced the chloro substituted of 1-phenylnaphthalene. The reaction yield was always high, and for many examples, it was only slightly affected by the aryl substituent. It is reported that this is related to results obtained with metalloporphyrins, which give lower selectivity due to the presence of variable amounts of triphenylbenzenes (figure 1).[15]

Herein, we report a smooth one-pot, solvent-free catalytic dimerization of phenylacetylene **1** (H-C≡C-Ph) to 1-phenylnaphthalene **2** by Cu/C in darkness and at room temperature in good yield (∼100%). The computational method employed covers density functional theory (DFT) approaches. The structure of **2** was optimized by DFT-B3LYP/6-31G* method. The barrier rotation around C-C of the phenyl and naphthalene parts of the molecule and its UV-Visible spectrum were calculated by B3LYP/6-31G* method. The modelling of the mechanism of formation of 1-phenylnaphthalene from phenylacetylene was performed with and without Cu/C catalyst. In this study, the data of EDS and SEM of the Cu/C catalyst surface are reported as well.

2. Experimental

2.1 *Materials, methods and instruments*

The synthesized 1-phenylnaphthalene **2** is a known compound (with CAS# 605-02-7) and its physical data, infrared and ^{1}H-NMR spectra are essentially identical with that of authentic sample.[16] The FT-IR spectra were recorded on a Shimadzu FT-IR 8000 spectrometer. ^{1}H-NMR and ^{13}C-NMR spectra were determined on a 300 MHz Brüker spectrometer. The solvent for NMR recording was $CDCl_3$. The product was examined by GC-MS (figures S1 and S2 in Supplementary Information). GC and GC-MS analysis were performed on a Shimadzu QP5050A GCMS instrument, injector at 200°C; temperature program: 100°C (2 min), then 16°C per min till 250°C on a Zebron capillary column ZB-5 (0.25 μm thickness, 0.32 mm diameter, 30 m length). TLC experiment with $CHCl_3$-petroleum ether-acetone (1:1:1) on silica gel plate showed just one strong spot for **2** in comparison with the starting material **1**. No details are given about the by-products and only the final product was considered.

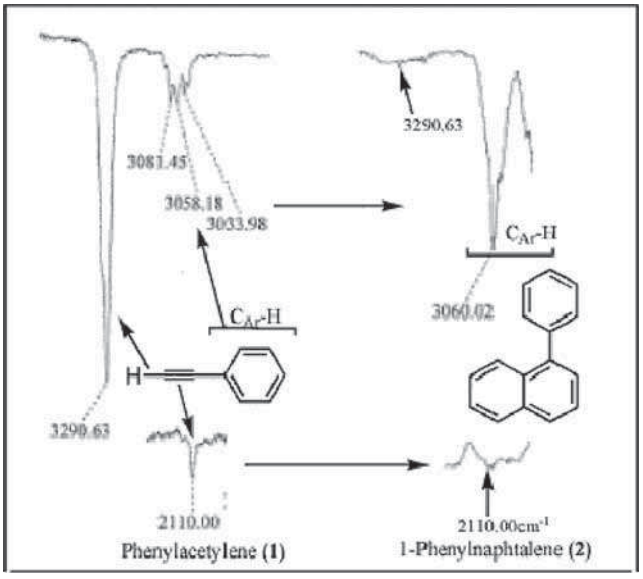

Figure 2. Comparison of FT-IR spectra of phenylacetylene **(1)** and 1-phenylnapthalene **(2)**. The peaks at 3291 and 2110 cm^{-1} have disappeared in spectrum of **2**.

2.2 *Procedures*

2.2a *Synthesis of 1-Phenylnaphthalene (2)*: A mixture of phenylacetylene **(1)** (2 mL, 1.86 g, 0.018 mol) and the catalyst Cu/C (0.1 mg) was made in a dried tube with a small magnetic stirrer bar. The tube was sealed and then stirred overnight (about 12 h) at room temperature and in darkness. A yellowish oily liquid was afforded after filtration and separation of the catalyst. The product **2** was identified by the analytical data and comparing with the authentic sample data.[16] The workup and GC yields were about ∼100% (2 mL, 1.85 g, 0.009 mol). See figures 2, S1 and S2 (S1 and S2 are in supplementary information.). B.p.: 322–324°C (lit. B.p.= 324–325°C).[16] FT-IR (KBr, cm^{-1}): 3000–3060(C-H; Ar.), 1812–2000(H-C; Ar. ring), 1594, 1487, 1443(C=C; Ar. ring), 780, 754 and 702 cm^{-1}(OOP of C-H; Ar. ring). ^{1}H-NMR δ_H($CDCl_3$): 7.87–7.91(m, H8), 7.83–7.85(m, H2), 7.51–7.53(m, H5), 7.48–7.50(m, H4), 7.47(d, H12, 6Hz), 7.45–7.47(dd, H3, 6Hz), 7.42(m, H7), 7.40(m, H6), 7.34–7.36(t, H13, 6Hz) and 7.30–7.32(d, H14, 6Hz). ^{13}C-NMR: 132.5(C11), 131.4(C1), 130.1(C10), 128.4(C9), 128.2(C13), 128.0(C8), 127.6(C5), 126.9(C4), 126.2(C14),

126.1(C12), 126.0(C7), 125.4(C6), 125.3(C2) and 125.2(C3). MS: m/z (relative intensity), MW=204; 204 (M^+, 94.9), 203(100), 202(60.5), 189(2.3), 176(4.5), 126(2.2), 102(8.1), 101(53.5), 88(18.6) and 76(10.5). Molecular formula is $C_{16}H_{12}$.

2.3 *Molecular Modeling*

The calculations on the structure of 1-phenylnaphthalene **2** were performed by appropriate quantum mechanical method. In this study, the employed computational method covers density functional theory (DFT) approaches. The structure of **2** was optimized by DFT-B3LYP/6-31G* method. All of the calculations have been performed by *Spartan '10* package that was implemented on a HP-Proliant-DL180-G6(12 cores) Server.[17] The graphing operation for barrier rotation ($\phi_{10,1,11,16}$) around C1-C11 in **2** was performed using the *Microsoft Office Excel-2013* program.

Figures 3 to 9 and table 1 show the appropriate model, operations and selected structural data. To calculate the barrier rotation around the C-C bond in 1-phenylnaphthalene (on Cu/C catalyst) the appropriate dihedral angle change ($\phi_{10,1,11,16}$) around the C1-C11 bond was utilized and optimized in each step. The *Hartree* energy was converted to kcal.mol^{-1} and relative energies were calculated. The graph in figure 4 demonstrates the appropriate data. The optimized structures of 1-phenylnaphthalene, transition states and intermediate (with and without Cu/C catalyst pathways) were carried out by DFT-B3LYP/6-31G* method.

Figure 3 demonstrates the selected structural data of **2** in ground state ($\phi_{10,1,11,16} = 90.52°$) and the barrier form ($\phi_{10,1,11,16} = 0°$). The steric restraint and the strains in the barrier form have made some changes in bond lengths and bond angles as compared to the ground state form. By increasing the steric restraint and the strains in the barrier form, the bond length of C1-C11, H23-H24 and H17-H24 were changed from 1.497, 3.416 and 3.524Å (in ground state) to 1.523, 0.899 and 1.787Å (in barrier form), respectively. Likewise, by increasing the steric restraint and the strains in the barrier form, the bond angles of C2C1C10, C10C1C11, C1C11C12 and C12C11C16 were changed from 119.4, 121.0, 120.7 and 118.0°(in ground state) to 118.2, 123.1, 122.1 and 116.8 (in barrier form), respectively. The barrier energy for bond rotation around$\phi_{10,1,11,16}$ was calculated 52.92 kcal mol^{-1} by B3LYP/6-31G* method (figure 4).

Figure 5(a) shows the calculated UV/Visible spectra for **2**. The calculated λ_{max} in vacuum by DFT-B3LYP/6-31G* method was achieved 269.2 nm (lit λ_{max} = 285 nm in n-hexane). The energies of the boundary MOs (HOMO and LUMO) of **2** are shown in Figure 5(b). The HOMO, LUMO and $\Delta E_{\text{HOMO-LUMO}}$ were calculated as: -5.73, -0.96 and 4.77 eV, respectively.

Figure 6 demonstrates the predicted mechanism of reaction between two moles of phenyl-acetylene to produce 1-Phenylnaphthalene **2**. The transition states (TS_1 and TS_2) and also the intermediate for a [1,5]H-shift are shown in figure 6. The hydrogen atom 19 has migrated from C10 to C4 by a [1,5]H-shift (sigma tropic) reaction. Table 1 shows the selected structural data of the structures during the production of **2** calculated by B3LYP/6-31G* method. The bond lengths and distances between the selected atoms C1-C2, C2-C3, C3-C4, C4-C5, C5-C10, C1-C10, C1-C11, C10-H19, H17-H18 and H18-H19 are: 1.295, 2.419, 1.277, 1.430,

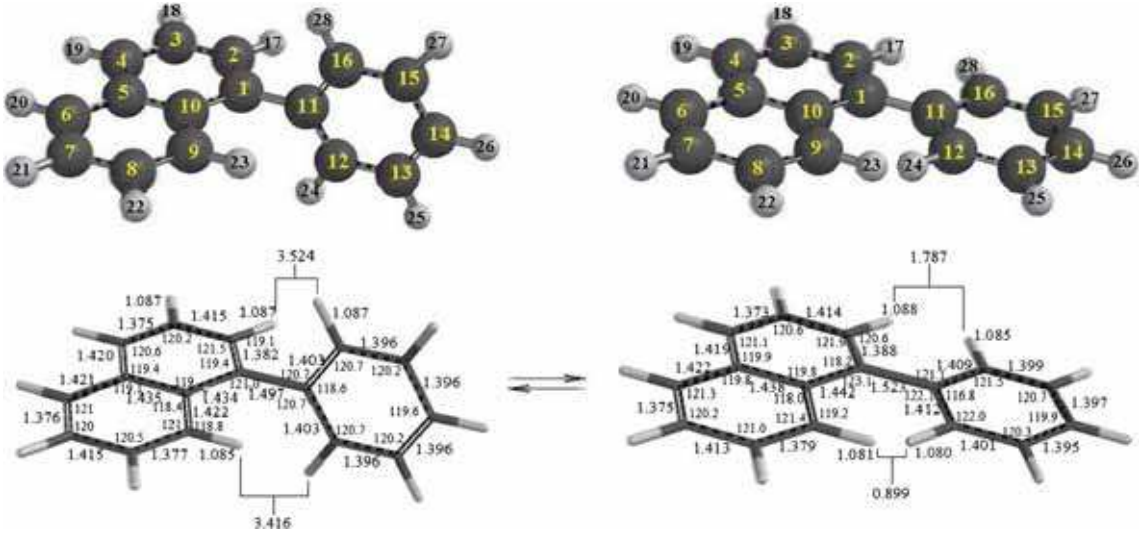

Figure 3. The selected structural data of 1-Phenylnaphthalene **(2)** in ground state ($\Phi_{10,1,11,16} = 90.52°$) and the barrier form ($\Phi_{10,1,11,16} = 0°$).

Table 1. Selected structural data of the transition states [TS_1], [TS_2] and the intermediate compound [In.].

	[TS_1] & [TS_2] and [In.]		
Selected data	[TS_1]	[In.]	[TS_2]
Bond length(Å)			
C1-C2	1.295	1.372	1.368
C2-C3	2.419	1.444	1.432
C3-C4	1.277	1.359	1.408
C4-C5	1.430	1.356	1.418
C5-C6	1.403	1.428	1.432
C5-C10	1.404	1.564	1.520
C9-C10	1.389	1.489	1.499
C1-C10	2.802	1.504	1.502
C1-C11	1.426	1.482	1.480
C2-H17	1.071	1.088	1.090
C3-H18	1.07 4	1.091	1.095
C10-H19	1.082	1.115	1.457
H17-H18	3.114	2.527	2.419
H18-H19	4.352	4.472	2.585
Bond angle(°)			
C1C2C3	126.92	119.56	122.01
C2C3C4	76.27	119.73	127.24
C3C4C5	170.12	124.41	116.13
C4C5C6	124.08	129.34	118.76
C4C5C10	116.64	117.52	125.45
C2C1C10	103.78	119.77	117.35
C2C1C11	159.81	120.60	121.68
C10C1C11	96.39	119.55	120.88
C5C10C1	78.62	115.12	116.31
C5C10H19	122.10	91.69	71.79
C1C10H19	92.98	102.56	90.25
C1C2H17	144.51	119.13	118.52
C4C3H18	154.25	121.78	118.42
Torsional angle(°)			
C1C2C3C4	27.39	−24.28	3.80
C2C3C4C5	−17.79	14.26	1.88
C3C4C5C6	120.51	−174.76	169.37
C3C2C1C10	−3.97	17.97	0.16
C3C4C5C10	−55.29	1.15	−11.72
C4C5C10H19	−19.01	−111.58	−65.84
C2C1C10C5	−42.17	−2.92	−8.58
C2C1C10H19	79.99	95.00	61.32
H17C2C3H18	34.19	−21.98	1.03
C5C10C1C11	138.66	−179.52	174.76

1.404, 2.802, 1.426, 1.082, 3.114 and 4.352 Å, respectively. For the intermediate [In.], the bond lengths and distances between the selected atoms C10-H19, C1-C10, C5-C10 and C1-C11 are: 1.115, 1.504, 1.564 and 1.482, respectively. In table 1 are shown, as well as [TS_1] and [In.] the selected bond lengths and distances C10-H19, C1-C10, C5-C10 and C1-C11 for [TS_2]: 1.457, 1.502, 1.520 and 1.480 Å, respectively. The calculated energy levels of the [In.] and [TS_2] by B3LYP/6-31G* method, are: 8.09 and 27.13 kcal mol^{-1}, respectively, less stable than the precursor. The calculated energy level of the product **2** is about 98 kcal mol^{-1} more stable than the precursor **1** (figure 7).

Figure 7 shows the graph of the reaction between two moles of **1** to produce one mole **2** with and without Cu/C catalyst. With respect to the results, the first step of this reaction was slow and rate determining. The activation energy of the first step was calculated to be about 107.42 kcal mol^{-1} without Cu/C catalyst. This activation energy for the first step and with Cu/C catalyst was about 66.66 kcal mol^{-1} by B3LYP/6-31G* method. The results show that the activation energy of this stage (by utilizing Cu/C catalyst pathway) decreases by about 41 kcal mol^{-1}. The results demonstrate that the slow and first step of this reaction was affected by the adsorption of phenylacetylene and the [TS_1] on Cu/C catalyst surface. An imaginary structure of Cu surface was constructed and optimized by B3LYP/6-31G* method, to construct a model for adsorbing two molecules of **1** and their [TS_1] on Cu/C catalyst surface. This model of Cu surface includes 64 Cu atoms (8x8) with 24.60 Å diagonal and 17.84 Å length. The optimized Cu-surface shows a curvature across its diagonal. Figure 8 shows the model of Cu-catalyst surface by B3LYP/6-31G* method: **(a)** Ball and spoke model, **b)** Electron density model, **c)** Electrostatic potential model with natural charges and **d)** Mulliken Charge map. The calculated results demonstrate that the Mulliken and natural charges have not been homogenized on the selected Cu-surface. The natural charge map of the optimized Cu-surface is shown in figure 4(C); the natural charges were changed from +0.055 to −0.048 esu. The most positive places are shown by blue color in figure 4(C) with +0.055 to +0.040 esu. It seems that these positions are better locations to adsorb the electron density distribution (EDD) of the first step transition state (TS_1) among the selected Cu-surface. So, these positions were chosen for modelling of this stage with Cu-catalyst with the phenylacetylene molecules. Figure 9 (**a** and **b**) presents the model of interaction between [TS_1] and the Cu-catalyst surface (**(a)** Space filling and **(b)** ball and spoke models). In this figure, we can obviously see the changes about the Cu atom positions of the Cu-model catalyst due to adsorption of the [TS_1]. As mentioned above the calculated results by the modelling show that the activation energy of this stage (by utilizing Cu/C catalyst pathway) to decrease by about 41 kcal mol^{-1}.

2.4 *EDS and SEM Results*

Figure S3 (in SI) shows the EDS results. This figure shows the copper atoms in the Cu/C catalyst. The

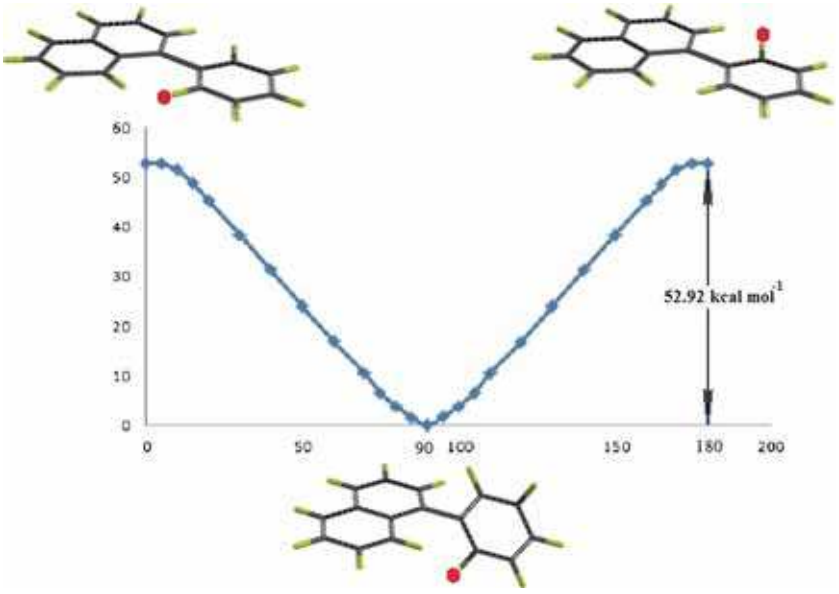

Figure 4. The rotation process in 1-phenylnaphthalene **(2)** in ground state ($\Phi_{10,1,11,16} = 90.52°$) and the barrier form ($\Phi_{10,1,11,16} = 0°$).

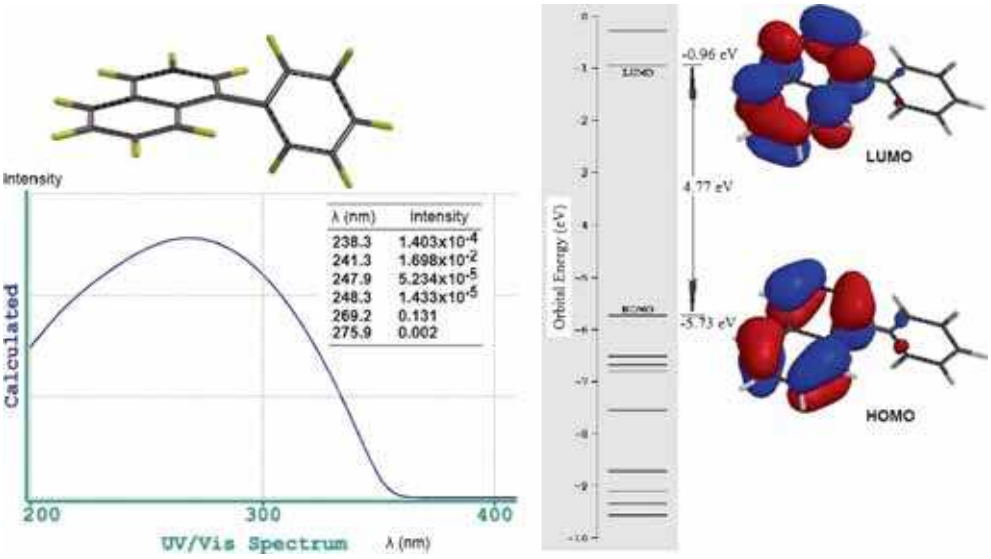

(a) (b)

Figure 5. **(a)** The calculated UV/Visible spectrum for 1-phenylnaphthalene **(2)**. Calculated λ_{max} =269.2 nm in vacuum by DFT-B3LYP/6-31G* method (lit. λ_{max} = 285 nm in nhexane). **(b)** The energies of MOs (HOMO and LUMO) of 1-phenylnaphthalene **(2)**.

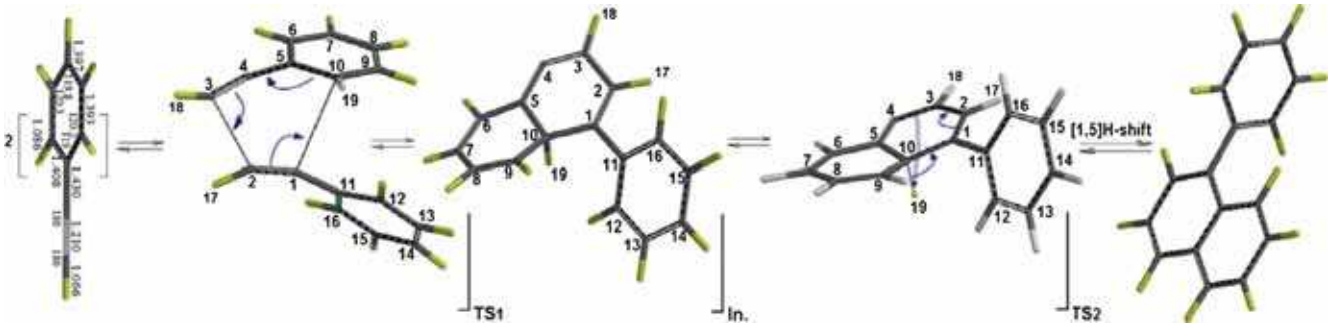

Figure 6. The predicted mechanism of reaction between two moles of phenylacetylene **(1)** to produce one mole of 1-phenylnaphthalene **(2)**.

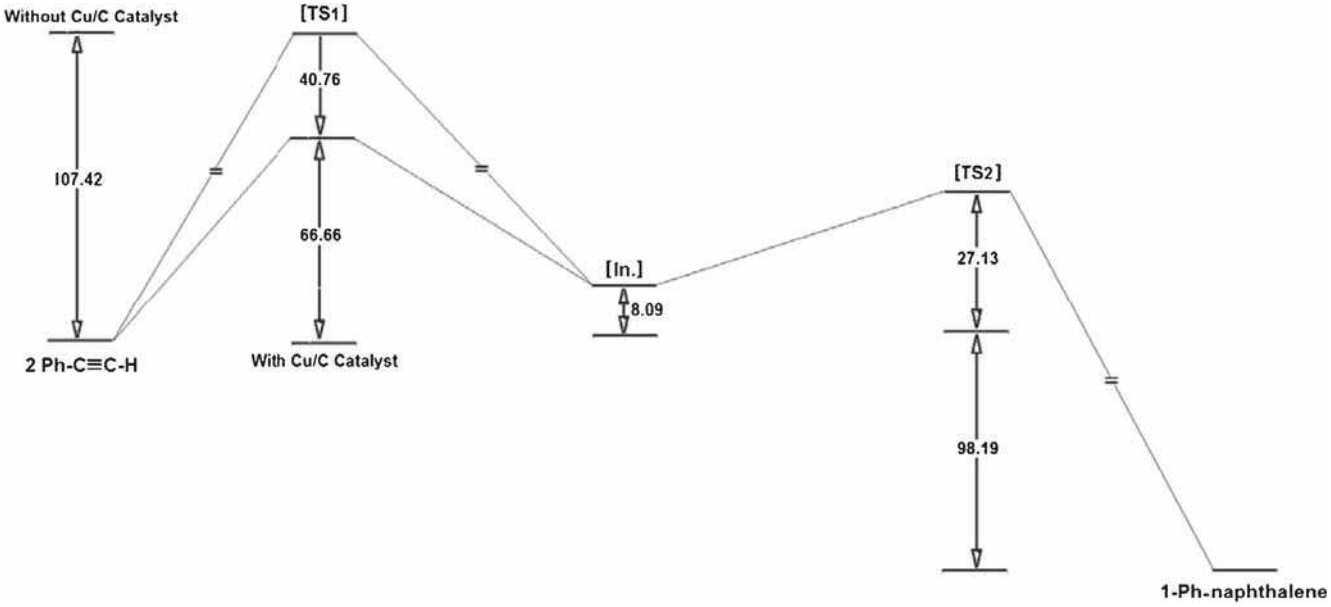

Figure 7. The graph of the reaction of two moles of phenylacetylene to produce 1-Ppenylnaphthalene **(2)** with and without catalyst Cu/C. With catalyst, the activation energy of the first step was calculated to be about 41 kcal mol^{-1} less than without Cu/C catalyst.

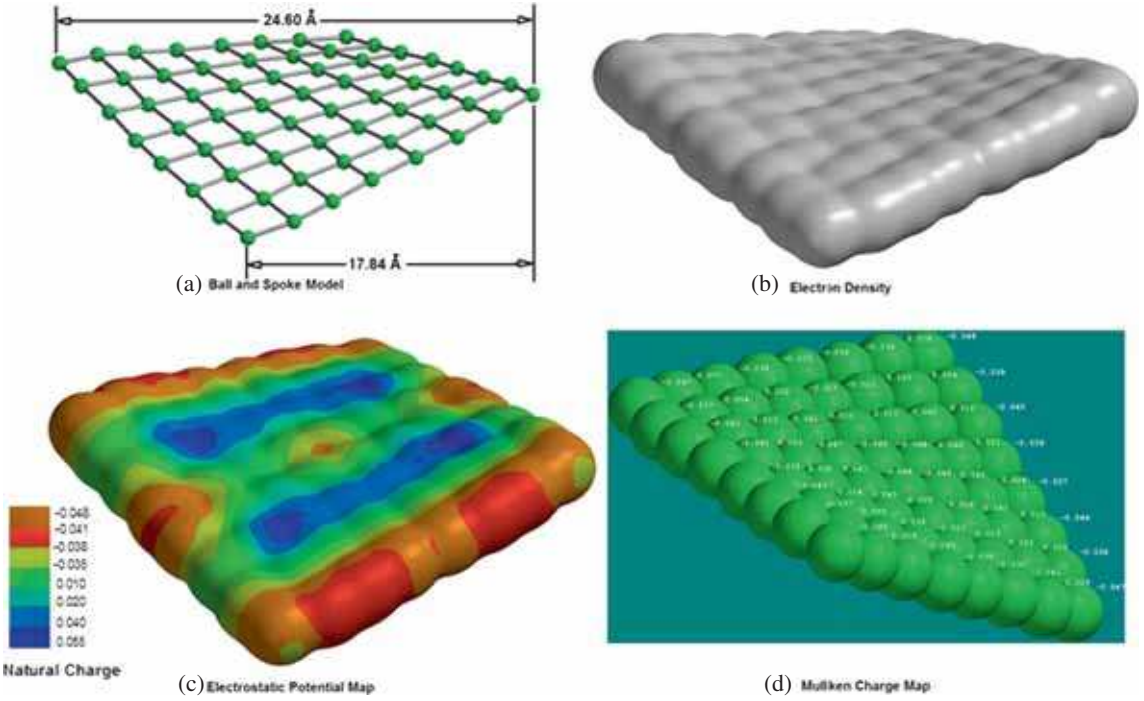

Figure 8. The calculated model of Cu-catalyst surface by B3LYP/6-31G* method. **a)** Ball and spoke model, **b)** Electron density model, **c)** Electrostatic potential model with natural charges and **d)** Mulliken Charge map.

results of electron microscopy image of the copper-impregnated carbon (Cu/C) sample with shows that the structure of the SEM image (100 μm) of free copper consisting of homogenous and porous structure of Cu/C catalyst. Figures 10, S3 and S4 show the SEM images of copper-impregnated carbon (Cu/C) catalyst. The SEM images show the establishment and adhesion capability of chemical and physical characteristics and mechanics of the porous surface of copper metal particles (figure 11).

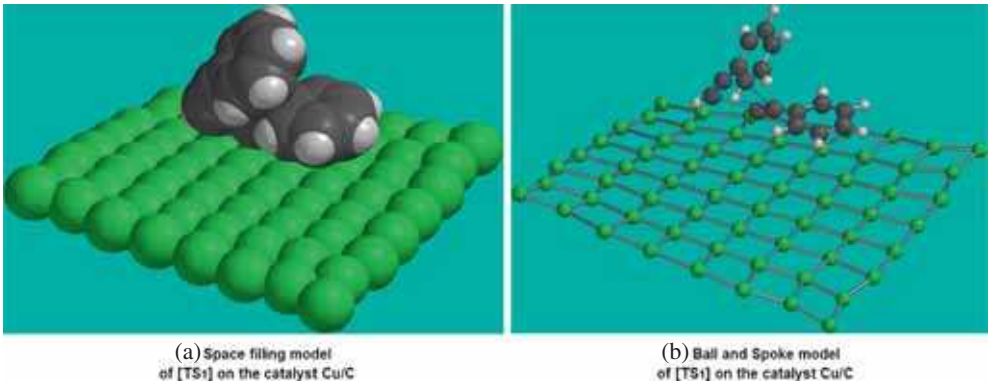

Figure 9. The model of interaction between **[TS_1]** and the Cu-catalyst surface. **(a)** Space filling and **(b)** ball and spoke models.

Figure 10. SEM image of copper-impregnated Carbon (Cu/C) catalyst in scale of 100 μm.

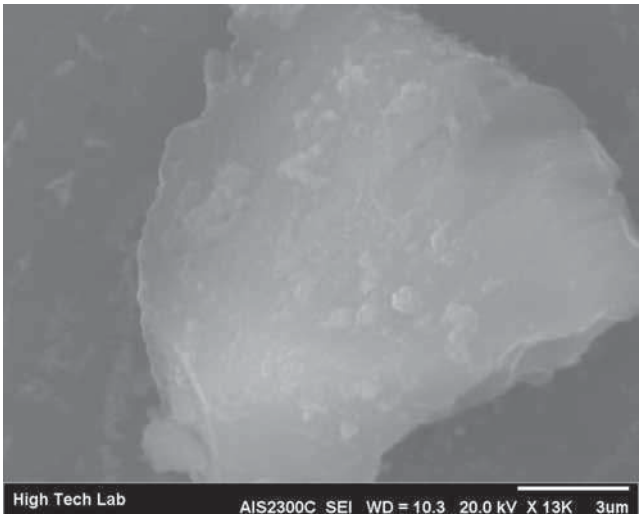

Figure 11. SEM image of copper-impregnated Carbon (Cu/C) catalyst in scale of 10 μm. See Figure 10.

3. Results and Discussion

The reaction was carried out as a one-pot, solvent-free catalytic dimerization of phenylacetylene **1** to 1-phenylnaphthalene **2** by Cu/C at room temperature and in good yield (~100%). The comparison of the structural and spectral data of **1** and the identified compound **2** shows complete conversion of **1** to **2** under the reaction conditions. There was no additional compound in the reaction vessel. The reactant vessel was under a dark cover during the time of reaction (overnight). So, the reaction was not under photochemical conditions.

The FT-IR spectrum of **1** has two important peaks at 2110 and 3291 cm^{-1} for stretching vibrational frequencies of –C≡C– and ≡C–H, respectively. These two signals disappeared in the FT-IR of the product **2**. The FT-IR of the product just shows the aromatic signals (figure 2). The ^{1}H-NMR spectrum of phenylacetylene showed a signal at chemical shift δ=2.16 ppm for acetylenic H atom. This signal disappeared completely in the ^{1}H-NMR spectrum of product **2.** The ^{1}H-NMR spectrum of **2** shows the NOE enhancement for H8 (peri-hydrogen) as doublet-multiplet by H7 and phenyl substituted group on C1 (figure S1 in supplementary information). The ^{13}C-NMR spectrum of **2** showed fourteen signals in accordance with its structure. A GC-Mass experiment was carried out on product **2**. The GC yield of the experiment was about ~100%. The mass spectrum of **2** showed the molecular weight $[M]^{+\cdot}$ signal at m/z=204. The signal of $[M]^{+\cdot}/2$ appeared at 102 and a signal at 101 for $([[M]^{+\cdot}/2)$-1] (figure S2 in supplementary information). The boiling point of the product was measured by Emrich's method.[15] The boiling point of **2** was 322–324°C (lit. B.p.= 324–325°C).[14] These results confirm conversion of **1** to **2** under the mentioned conditions.

4. Conclusions

A smooth one-pot, solvent-free catalytic dimerization of phenylacetylene to 1-phenylnaphthalene by Cu/C in darkness at room temperature in good yield (∼100%) is reported. The identification of the product was carried out by the physical data, FT-IR, ^{1}H-NMR, ^{13}C-NMR and mass spectra and compared with the authentic sample data. The structure of 1-phenylnaphthalene was optimized by DFT-B3LYP/6-31G* method. The barrier rotation around C-C of the phenyl and naphthalene parts of 1-phenylnaphthalene (52.92 kcal mol^{-1}) and its UV-Visible spectrum (λ_{max} =269.2 nm) were calculated by B3LYP/6-31G* method. The modelling of the production mechanism of 1-phenylnaphthalene from phenylacetylene was performed with and without Cu/C catalyst. The calculated results by the modelling showed that the activation energy (by utilizing Cu/C catalyst) decreases by about 41 kcal mol^{-1}. In this study, the data of EDS and SEM of the Cu/C catalyst surface are reported as well.

Supplementary Information

^{1}H-NMR spectra of phenyl-acetylene, 1-phenylnaphthalene (figures S1 and S2), EDS analysis (figure S3) and the SEM of Cu/C catalyst (figure S4) are shown in the Supplementary Information which is available at www.ias.ac.in/chemsci.

Acknowledgements

A T gratefully acknowledges the colleagues in Chemistry Department of The University of Queensland-Australia for their useful suggestions. The authors are grateful to the Research and Computational Lab of Theoretical Chemistry and Nano Structures of Razi University Kermanshah-Iran for supporting this study.

References

1. Fetzer J C 2000 *Polycycl. Aromat. Comp.* **27** 143
2. Herwig P T, Enkelmann V, Schmelz O and Müllen K 2000 *Chem. Eur. J.* **6** 1834
3. Glenn R M 1995 In *Activated carbon applications in the food and pharmaceutical industries* (Boca Raton FL: CRC Press) p. 125
4. Portella G, Poater J and Solà M 2005 *J. Phys. Org. Chem.* **18** 785
5. Luch A 2005 In *The Carcinogenic Effects of Polycyclic Aromatic Hydrocarbons* (London: Imperial College)
6. Hawley G G 1997 In *Condensed Chemical Dictionary* 13th Ed. (New York: Van Nostrand Reinhold Company Inc.)
7. (a) Weiss R 1955 *Org. Syntheses* **3** 729; (b) Chattaway F D 1893 *J. Chem. Soc.* **63** 1187; (c) Weiss R and Woidich K 1925 *Monatsh. Chem.* **46** 455; (d) Cook J W and Lawrence C A 1936 *J. Chem. Soc.* **11** 1431; (e) Vesely V and Stursa F 1933 *Collect. Czech. Chem. Commun.* **5** 344; (f) Orchin M and Reggel L 1947 *J. Am. Chem. Soc.* **69** 505; (g) Grieve W S M and Hay D H 1938 *J. Chem. Soc.* **13** 108; (h) Waters W H 1939 *J. Chem. Soc.* **14** 864; (i) Hodgson H H and Marsden E 1940 *J. Chem. Soc.* **15** 208; (j) Bachmann W E and Hofmann R A 1944 *Org. Reac.* **2** 248
8. Sun C L, Li H, Yu D G, Yu M, Zhou X, Lu X Y, Huang K, Zheng S F, Li B J and Shi Z J 2010 *Nature Chem.* **2** 1044
9. Firouzabadi H, Iranpoor N and Ghaderi A 2011 *Org. Biomol. Chem.* **9** 865
10. Sonogashira K, Tohda Y and Hagihara N 1975 *Tetrahedron Lett.* **16** 4467
11. Chinchilla R and Najera C 2007 *Chem. Rev.* **107** 874
12. Gil-Molto J and Najera C 2006 *Adv. Synth. Catal.* **348** 1874
13. Dudnik A and Gevorgyan V 2010 *Angew. Chem. Int. Ed.* **49** 2096
14. Cicero D, Lembo A, Leoni A and Tagliatesta P 2009 *New J. Chem.* **33** 2162
15. Vogel A 1986 In *Vogel's Textbook of Practical Organic Chemistry*. *Including qualitative organic analysis* (4th Ed). (England: Longman Group Limited)
16. (a) Pouchert C L 1983 In *The Aldrich Library of NMR Spectra* (2th Ed.). (Milwaukee, Wisconsin: Aldrich Chemical Company Inc.) **1** pp. 2, 740-2, 762; (b) Pouchert C L 1981 In *The Aldrich Library of Inferared Spectra* 3th Ed. (Milwaukee, Wisconsin: Aldrich Chemical Company Inc.) pp. 27, 40-2, 578; (c) 1-phenylnaphthalene http://www.chemsynthesis.com/base/chemical-structure-5127.html
17. *Spatran '10*-Quantum Mechanics Program: (PC/x86) 1.1.0 v4. 2011 (Irvine CA: Wavefunction Inc.)